The Journal of Immunology

Neonatal Fc Receptor Blockade by Fc Engineering Ameliorates Arthritis in a Murine Model

Dipesh A. Patel, Alberto Puig-Canto, Dilip Kumar Challa, Héctor Perez Montoyo, Raimund J. Ober and E. Sally Ward

J Immunol 2011; 187:1015-1022; Prepublished online 20 June 2011;
doi: 10.4049/jimmunol.1003780
http://www.jimmunol.org/content/187/2/1015

The Journal of Immunology is published twice each month by
The American Association of Immunologists, Inc.,
9650 Rockville Pike, Bethesda, MD 20814-3994.

Print ISSN: 0022-1767 Online ISSN: 1550-6606.

Neonatal Fc Receptor Blockade by Fc Engineering Ameliorates Arthritis in a Murine Model

Dipesh A. Patel,*,[1] Alberto Puig-Canto,*,[1] Dilip Kumar Challa,* Héctor Perez Montoyo,*,[2] Raimund J. Ober,*,† and E. Sally Ward*

Multiple autoimmune diseases are characterized by the involvement of autoreactive Abs in pathogenesis. Problems associated with existing therapeutics such as the delivery of intravenous immunoglobulin have led to interest in developing alternative approaches using recombinant or synthetic methods. Toward this aim, in the current study, we demonstrate that the use of Fc-engineered Abs (Abs that enhance IgG degradation [Abdegs]) to block neonatal FcR (FcRn) through high-affinity, Fc region binding is an effective strategy for the treatment of Ab-mediated disease. Specifically, Abdegs can be used at low, single doses to treat disease in the K/B×N serum transfer model of arthritis using BALB/c mice as recipients. Similar therapeutic effects are induced by 25- to 50-fold higher doses of i.v. Ig. Importantly, we show that FcRn blockade is a primary contributing factor toward the observed reduction in disease severity. The levels of albumin, which is also recycled by FcRn, are not affected by Abdeg delivery. Consequently, Abdegs do not alter FcRn expression levels or subcellular trafficking behavior. The engineering of Ab Fc regions to generate potent FcRn blockers therefore holds promise for the therapy of Ab-mediated autoimmunity. ***The Journal of Immunology*****, 2011, 187: 1015–1022.**

Although the focus of therapeutic approaches for autoimmunity has in the past been on targeting cellular immunity, considerable recent interest has been directed toward the humoral component for diseases in which Abs play a role in pathogenesis (1, 2). In many cases, current therapies for Ab-mediated diseases, such as systemic lupus erythematosus and myasthenia gravis, involve the use of immunosuppressive drugs or steroids, which have undesirable side effects (3, 4). Although high doses of intravenous immunoglobulin (IVIG) can be effective in ameliorating inflammatory diseases (5, 6), the use of this reagent can result in adverse events, such as immune complex-mediated damage (7, 8). Currently, there is also a worldwide shortage of IVIG (9). These shortcomings motivate the use of recombinant or synthetic approaches to develop new treatments.

A strategy that has recently been advocated to treat Ab-mediated autoimmunity is to design reagents that can lower Ab levels in vivo (10–12). This is of particular relevance because B cell depletion using Abs to target CD20 does not lower the levels of autoreactive IgGs sufficiently to modulate autoantibody-mediated disease due to the lack of CD20 expression by long-lived plasma cells (1, 13). It is well established that the MHC class I-related receptor, neonatal FcR (FcRn), regulates the levels and transport of Abs throughout the body (14–16). The inhibition of this receptor therefore provides a possible target for the therapy of IgG-mediated autoimmune diseases (10–12, 17–19). However, the ability of relatively low and single doses of FcRn blockers to ameliorate such diseases is uncertain. In addition, whether FcRn blockade alone is effective in treating Ab-mediated disease is a major issue regarding the feasibility of this strategy. For example, it is unclear whether other anti-inflammatory pathways, such as those involving FcγRIIB upregulation (20, 21), are necessary for therapeutic benefit. This question has been prompted by studies using high-dose IVIG to treat inflammatory disease: some studies support a role for FcRn blockade in the reduction of disease activity (19, 22, 23), whereas others have reported that the beneficial effects of IVIG are solely due to upregulation of the inhibitory FcγR, FcγRIIB (20, 21), or a combination of pathways involving both FcRn and FcγRIIB (24). Resolution of this issue is critical for the design of therapeutics for targeting Ab-mediated inflammatory disease.

Toward the goal of inhibiting FcRn function, we have recently described a class of Abs called Abdegs (Abs that enhance IgG degradation) that are engineered to bind with increased affinity to FcRn through their Fc region at both acidic and near neutral pH (10, 25). To date, however, the activity of Abdegs in treating Ab-mediated disease is untested. Wild-type Abs bind with very low affinity to FcRn at near neutral pH and are dependent on fluid-phase uptake for entry into cells, whereas Abdegs enter cells primarily by receptor-mediated processes (10, 26). Consequently, Abdegs compete very effectively with wild-type IgGs for FcRn interactions because they not only bind more strongly to this receptor at endosomal pH, but also accumulate within cells to much higher concentrations (10, 25). As such, these engineered Abs have a major competitive advantage for FcRn binding over existing lower-affinity, wild-type inhibitors such as IVIG. The binding properties of an Ab for FcRn also impact its in vivo $t_{1/2}$, with gain of binding at pH 7.4 resulting in lysosomal accumulation and lower in vivo persistence (25, 27, 28). Consequently, the competitive ability and in vivo $t_{1/2}$ of an Abdeg can be tuned for specific applications (16).

In this study, we have used a murine model of rheumatoid arthritis [via transfer of K/B×N serum (29)] to both analyze the

*Department of Immunology, University of Texas Southwestern Medical Center, Dallas, TX 75390-9093; and †Department of Electrical Engineering, University of Texas at Dallas, Richardson, TX 75080

[1]D.A.P. and A.P.-C. contributed equally to this work.

[2]Current address: Centro de Investigación Príncipe Felipe, Valencia, Spain.

Received for publication November 22, 2010. Accepted for publication May 13, 2011.

This work was supported in part by Grants RO1 AR 56478 and R01 AI 39167 from the National Institutes of Health (to E.S.W.).

Address correspondence and reprint requests to Dr. E. Sally Ward, Department of Immunology, University of Texas Southwestern Medical Center, 6000 Harry Hines Boulevard, Dallas, TX 75390-9093. E-mail address: sally.ward@utsouthwestern.edu

Abbreviations used in this article: Abdegs, Abs that enhance IgG degradation; FcRn, neonatal FcR; GPI, glucose-6-phosphate isomerase; IVIG, intravenous immunoglobulin; SNA, *Sambucus nigra* agglutinin.

www.jimmunol.org/cgi/doi/10.4049/jimmunol.1003780

therapeutic activity of Abdegs and address the fundamental question as to whether FcRn blockade without other contributing anti-inflammatory effects can alleviate ongoing, IgG-mediated disease. In this model, arthritis develops in normal mice following the transfer of anti–glucose-6-phosphate isomerase (anti-GPI) Abs that complex with endogenous GPI (30). These immune complexes infiltrate joints, where they initiate an inflammatory cascade within minutes following transfer (31–33). This model is therefore instructive for the analysis of therapies that target the humoral response. We demonstrate that Abdegs can effectively treat arthritis through a mechanism involving FcRn inhibition. Collectively, our observations indicate that the use of Fc-engineered Abs of the Abdeg class holds considerable promise for the treatment of arthritis, and by extension, other diseases in which Abs play a role in pathology.

Materials and Methods

Mice

K/B×N mice were generated by intercrossing KRN TCR transgenic mice (provided by C. Benoist and D. Mathis) with NOD mice (29). Offspring were typed by flow cytometric analysis of lymphocytes in the blood using an anti-Vβ6 Ab that recognizes the TCRβ chain of the transgene (29). Sera were harvested from 8- to 10-wk-old $V\beta6^+$ K/B×N mice for use in transfer experiments. BALB/c and FcRn knockout mice (34) were purchased from The Jackson Laboratory (Bar Harbor, ME). All animal protocols have been approved by the Institutional Animal Care and Use Committee at the University of Texas Southwestern Medical Center (Dallas, TX).

Antibodies

Wild-type human IgG1 and the mutant MST-HN (Met^{252} to Tyr, Ser^{254} to Thr, Thr^{256} to Glu, His^{433} to Lys, and Asn^{434} to Phe) are both specific for hen egg lysozyme and were purified using lysozyme-Sepharose (10, 35). To generate MST-HN + N297A, an Ab H chain expression construct encoding the MST-HN mutant in combination with N297A (to express in aglycosylated form) was transfected into a L chain-expressing NSO cell line (35). Ab-expressing clones were identified and expanded for protein expression, as described (10, 35). Binding properties of purified human IgG1 and MST-HN for FcRn were confirmed using surface plasmon resonance (BIAcore) (36) prior to use in vivo. IVIG (Gammunex) was obtained at 100 mg/ml from Talecris. The mouse anti-lysozyme Ab, D1.3 (37), was purified using lysozyme-Sepharose.

Effect of MST-HN and IVIG on the clearance of radiolabeled IgG1

The effect of the MST-HN mutant on the clearance of ^{125}I-labeled wild-type mouse IgG1 (D1.3) was determined, as described (10). Drinking water was supplemented with 0.1% Lugol 72 h before radiolabeled mouse IgG1 was injected i.p. into BALB/c mice, and radioactivity was monitored at the indicated times by whole-body counting (25) (Atom Lab 100 Dose Calibrator). Seventy-two hours later, mice were i.v. injected with either PBS, 0.5, 1, or 2 mg MST-HN, and whole-body radioactivity was determined at the indicated times. Similarly, the effect of IVIG on the clearance of D1.3 was compared with that of MST-HN using an analogous approach, except that 72 h postdelivery of radiolabeled D1.3, mice were i.v. injected with either 1 mg wild-type IgG1 or MST-HN, or 25 or 50 mg IVIG, and whole-body counts were determined at the indicated times.

To analyze the effect of MST-HN on the clearance of mouse IgG1 in FcRn-deficient mice (34), mice were treated as above, except that a dose of 1 mg MST-HN or wild-type IgG1 was injected into FcRn-deficient mice 15–20 min following the i.v. delivery of radiolabeled mouse IgG1 (D1.3). β-phase $t_{1/2}$ values of radiolabeled D1.3 were determined by fitting the data to a decaying biexponential model using MATLAB (Mathworks) and custom written software (38).

Appearance of i.p. injected mouse IgG1 in the blood

Mouse IgG1 (D1.3) was radiolabeled, as described (25). Following i.p. injection of the radiolabeled Ab, counts in 10 μl blood were determined at the indicated times by scintillation counting.

Serum-induced arthritis, therapy experiments, and prophylactic treatment

Sera harvested from arthritic K/B×N mice were analyzed for anti-GPI titers using ELISAs. On day 0, arthritis was induced in BALB/c recipients by i.p. delivery of 150 μl K/B×N serum. Six hours following serum delivery, mice were treated with i.v. injections (200–250 μl per mouse) of MST-HN, wild-type human IgG1, IVIG, or PBS at the doses indicated. In cases in which 50 mg IVIG was used, i.v. injections (250 μl each) were delivered twice, first at 6 h postserum transfer and then after an additional 3–4 h. Mice were also treated either 72 h following, or 12 h prior to, K/B×N serum transfer with i.v. injections of 1 mg/mouse MST-HN, wild-type IgG1, or PBS. Ankle and paw thicknesses were determined using an analog caliper (Dyer 313 series) by two independent observers.

Histopathology

Inflammatory cell infiltration into ankle joints was visualized in hindlimbs isolated from mice 6 d following serum delivery. BALB/c mice were injected i.p. with 150 μl K/B×N serum and after 6 h treated i.v. with either 1 mg/mouse MST-HN, wild-type human IgG1, or PBS. Mice were euthanized, and hindlimbs were skinned and fixed in 10% neutral buffered formalin for ~60 h. Following decalcification with Cal-Rite solution, tissue samples were embedded in paraffin wax, sagitally sectioned, deparaffinized, and stained with H&E. Slides were imaged and acquired using a Leica DM2000 upright photomicroscope (Leica Microsystems, Wetzlar, Germany) equipped with bright-field and epifluorescence optics and an Optronics Microfire color CCD camera (Optronics, Goleta, CA). A G4 Macintosh (OS 10.4.11) with Pictureframe 2.0 acquisition software was used to acquire and store images.

ELISAs to determine autoantibody, IgG, and albumin levels

Serum samples of BALB/c mice prior to induction of arthritis and after treatment were obtained via retro-orbital bleeding at the indicated times. These samples were used to determine anti-GPI Ab levels, total IgG levels, and albumin levels using sandwich ELISAs and serum dilutions of 1:500, 1:4,000, and 1:50,000, respectively. For measuring anti-GPI Ab levels, 1.25 μg/ml recombinant GPI (Roche) was used to coat 96-well plates, and bound Ab was detected using HRP rabbit anti-mouse IgG (H and L chain specific; Dako). IgG and albumin levels were determined using ELISA quantitation kits for mouse IgG and albumin (Bethyl Laboratories).

Lectin immunoblotting

A total of 1 μg each of recombinant Ab or IVIG was electrophoresed on 12% polyacrylamide gels with BenchMark Prestained protein ladder (Invitrogen). Electrophoresed proteins were either transferred onto a polyvinylidene difluoride membrane (Millipore; Immobilon-P) or stained with Coomassie brilliant blue. The membrane was incubated with 1% Western blocking reagent (Roche) for 1 h, followed by 1 μg/ml biotinylated Elderberry Bark Lectin (*Sambucus nigra* agglutinin [SNA]; Vector Laboratories) in Western blocking reagent for 1 h, and subsequently washed twice with TBS/0.1% Tween and once with TBS (pH 7.4). The membrane was then incubated with 2.25 μg/ml Extravidin-peroxidase conjugate (Sigma-Aldrich) in Western blocking reagent for 30 min prior to washing, as above. Bound SNA was detected by incubation with 0.6 mg/ml 3,3-diaminobenzidine tetrahydrochloride with 0.01% (v/v) hydrogen peroxide.

Statistical analyses

The n for each data set is indicated, and statistical significance for each time point was determined by ANOVA using MATLAB (Mathworks). ANOVA was carried out by paired comparisons between different mouse groups using the Tukey-Kramer test at a 95% confidence interval ($\alpha = 0.05$). Two-tailed Student t test was used to compare two treatment groups. The p values <0.05 were considered to be significant, and actual values are indicated. Outliers due to experimental artifacts were removed from the analyses. Data shown are mean values of treatment groups with error bars indicating SEs (SEM).

Results

Dose–response analysis of the effects of the MST-HN Abdeg on IgG levels

The current study is directed toward analyzing the therapeutic efficacy of a mutated human IgG1 (MST-HN, Met^{252} to Tyr, Ser^{254} to Thr, Thr^{256} to Glu, His^{433} to Lys, and Asn^{434} to Phe) (10) that is designed to inhibit FcRn function in a mouse model of Ab-

mediated arthritis. We initially investigated how the dose of MST-HN Abdeg impacts the levels of competing wild-type tracer IgG in vivo. BALB/c mice were used throughout these studies because this mouse strain is highly susceptible to arthritis following the transfer of arthritogenic serum derived from K/B×N mice (39). Mice were injected i.p. with radiolabeled mouse IgG1 and, 3 d later, 0.5, 1, or 2 mg MST-HN per mouse was delivered by i.v. injection. A dose of 0.5 mg per mouse (~25 mg/kg) induces a lower decrease in tracer IgG1 levels relative to 1 mg (~50 mg/kg) (Fig. 1). By contrast, comparison of doses of 1 and 2 mg MST-HN per mouse indicates no significant differences, demonstrating that for FcRn inhibition in BALB/c mice there is no advantage in using doses >1 mg per mouse (Fig. 1).

Dynamics of appearance of Abs in the circulation following i.p. delivery

Anti-GPI Abs, primarily of the IgG1 isotype, are known to be the mediators of disease in the K/B×N model (32). In the current experiments, we induced arthritis by transferring serum from arthritic K/B×N mice by i.p. delivery into BALB/c recipient mice. Prior to the delivery of potential therapeutics, initial analyses were therefore carried out to determine the time at which i.p. injected mouse IgG1 could be detected in the serum of BALB/c mice. The levels of radiolabeled IgG1 in the blood approach maximal levels at the earliest sampling point of 2 h, but continue to increase slowly to peak levels until 6 h postdelivery (Fig. 2). Positron emission tomography imaging has shown that anti-GPI Abs in the serum localize to joints at detectable levels within several minutes of delivery (33), indicating that extravasation to the target site is very rapid.

MST-HN is effective in ameliorating arthritis

The therapeutic effect of treatment with 0.5 or 1 mg MST-HN (per mouse) on arthritis was initially assessed by transferring arthritogenic serum into BALB/c mice and treating 6 h later. Mice were treated with MST-HN (0.5 or 1 mg), or as controls with wild-type IgG1 (0.5 or 1 mg; same binding specificity as MST-HN) or PBS vehicle. Disease severity was monitored by determining ankle and paw thickness. The data shown in Fig. 3*A* and 3*B* clearly demonstrate that MST-HN treatment at a time point when substantial accumulation of anti-GPI:GPI immune complexes in joints is expected (Fig. 2) (33) results in significantly lower disease activity relative to controls (wild-type IgG1 or PBS). Although both 0.5 mg (~25 mg/kg) and 1 mg (~50 mg/kg) MST-HN induce therapeutic effects, the higher dose is more effective in treating disease. In addition, there was no significant difference between wild-type IgG1 and PBS treatment groups (Fig. 3*A*, 3*B*). Similar results were observed when paw swelling was used to assess disease activity (data not shown). Delivery of MST-HN to mice following injection of control (nonarthritogenic) serum did not have any impact on joint size (data not shown), indicating the specificity of the effects on autoantibody-mediated disease.

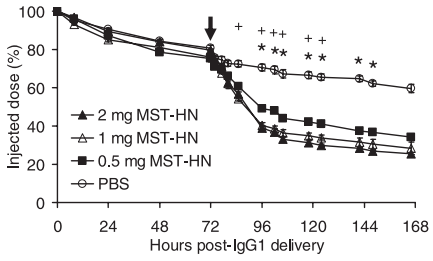

FIGURE 1. MST-HN shows a dose-dependent effect on tracer IgG1 levels. BALB/c mice were injected i.p. on day 0 with ^{125}I-labeled mouse IgG1. After 72 h (indicated by arrow), mice were injected i.v. with either 0.5, 1, 2 mg MST-HN, or PBS (n = 3 mice per treatment group). Levels of remaining radiolabeled mouse IgG1 were determined by whole-body counting at the indicated times. Radioactivity levels were significantly lower for all MST-HN treatment groups relative to the PBS treatment group from 85 to 166 h ($p < 2 \times 10^{-5}$; ANOVA). Relative to the 0.5 mg MST-HN treatment group, radioactivity levels were significantly lower in mice treated with 1 mg MST-HN ($+p < 2 \times 10^{-5}$, 85 h; $p < 3 \times 10^{-6}$, 96–124 h; ANOVA) or 2 mg MST-HN ($*p < 3 \times 10^{-6}$, 96–124 h; $p < 1.5 \times 10^{-6}$, 142–148 h; ANOVA). Differences between the 1 and 2 mg MST-HN treatment groups were not significant. Error bars indicate SEM. Data are representative of two independent experiments.

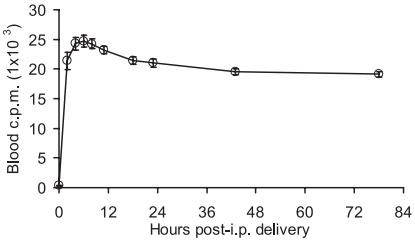

FIGURE 2. The appearance of i.p. delivered mouse IgG1 in the circulation of recipient mice peaks at 6 h postdelivery. Mice were injected i.p. with ^{125}I-labeled mouse IgG1, and radioactivity in blood samples was determined at the indicated times (n = 6 mice). Error bars indicate SEM. Data are representative of two independent experiments.

Histopathological analysis of ankle joints showed markedly less infiltration of immune cells in mice treated with MST-HN relative to mice in control treatment groups (Fig. 3*C*). As a result, no obvious bone damage was observed in MST-HN–treated mice, whereas mice treated with either wild-type IgG1 or PBS showed substantial inflammatory cell invasion and bone/tissue damage (Fig. 3*C*). We also determined the anti-GPI levels in sera of mice immediately prior to and following delivery of MST-HN (~50 mg/kg), wild-type IgG1, or PBS (Fig. 3*D*). Disease activity was found to correlate with anti-GPI Ab levels, with MST-HN treatment resulting in a rapid decrease in these Ab levels within several hours of delivery.

To further investigate the therapeutic effects of MST-HN, we analyzed whether MST-HN delivery during established disease (3 d postserum transfer) ameliorated arthritis. Relative to control groups, MST-HN treatment resulted in a rapid attenuation of disease (Fig. 4*A*). In addition, we determined the effect of administration of MST-HN prior to K/B×N serum transfer. Prophylactic treatment with MST-HN 12 h prior to K/B×N serum transfer resulted in less severe disease relative to that observed in wild-type IgG1-treated mice (Fig. 4*B*). However, the reduction was not as pronounced compared with the effect of Abdeg delivery 6 h posttransfer of arthritogenic serum (Fig. 3*B*).

The therapeutic effect of MST-HN on disease involves FcRn blockade

Earlier studies have indicated that sialylation through α2,6 linkage to the *N*-linked carbohydrate, present on 1–3% of IgG molecules in IVIG preparations, mediates anti-inflammatory effects by inducing the upregulation of FcγRIIB (20, 21, 40). It was therefore important to determine whether similar effects could contribute to disease amelioration induced by MST-HN. Immunoblotting with a lectin (SNA) specific for α2,6-linked sialic acid indicated that MST-HN, wild-type IgG1, and IVIG all bear similar levels of this type of sialic acid (Fig. 5). A possible contribution of this sialic acid form to the anti-inflammatory effects of MST-HN was therefore directly assessed by comparing the activity of this Ab with its parent, wild-type counterpart. Significantly, our

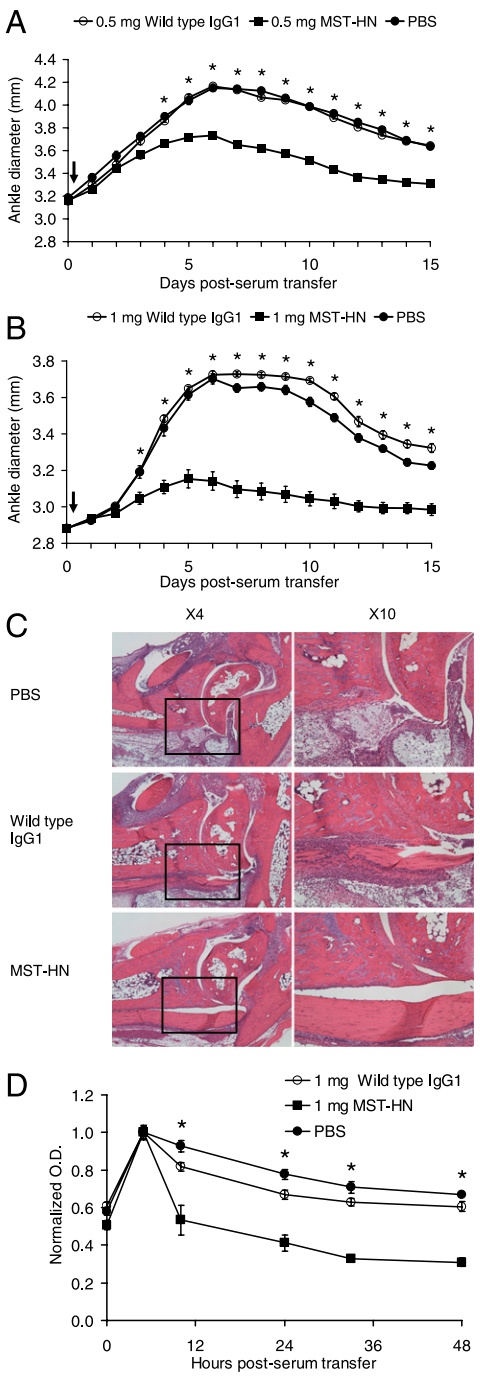

FIGURE 3. MST-HN is effective in treating arthritic mice. *A*, BALB/c mice were injected on day 0 with arthritogenic serum and 6 h later (indicated by arrow) treated with 0.5 mg MST-HN, 0.5 mg wild-type IgG1, or PBS (n = 6 mice per treatment group). Ankle swelling (both ankles analyzed for each mouse) was not significantly different between wild-type IgG1- and PBS-treated mice, whereas MST-HN treatment significantly reduced swelling with respect to wild-type IgG1 or PBS treatment from day 4 onward (all $*p < 2 \times 10^{-7}$; ANOVA). *B*, Mice were treated and analyzed, as described in *A*, but 1 mg MST-HN, 1 mg wild-type IgG1, or PBS (n = 6 mice per treatment group) was administered. Ankle swelling in MST-HN–treated mice was significantly lower compared with that for either wild-type IgG1- or PBS-treated mice from day 3 onward ($*p < 1 \times 10^{-2}$, day 3; all $p < 1 \times 10^{-8}$, day 4 onward; ANOVA). No significant difference was observed between wild-type IgG1 and PBS treatment groups. *C*, Mice (n = 4 per treatment group) were treated, as described in *B*, and hindlimbs were harvested 6 d after K/B×N serum delivery. Limbs were subsequently skinned, fixed, decalcified, and embedded in paraffin wax before 5-μm–thick sections were cut. Ankle joint sections were stained with H&E. Sections shown are at original magnification ×4 and ×10 (black box in original magnification ×4 images indicates region observed at original magnification ×10). Images are representative of each treatment group. *D*, Mice were treated as described in *B*, and anti-GPI Ab levels in sera of mice (4–6 mice per treatment group; duplicate samples for each mouse) were determined by ELISA before and following treatment. Serum anti-GPI levels were significantly lower at the indicated times (*) in MST-HN–treated mice compared with mice treated with PBS or wild-type IgG1 ($p = 6.7 \times 10^{-7}$, 10 h; $p = 2.8 \times 10^{-9}$, 24 h; $p = 1.4 \times 10^{-9}$, 33 h; $p = 9 \times 10^{-9}$, 48 h; ANOVA). Error bars indicate SEM.

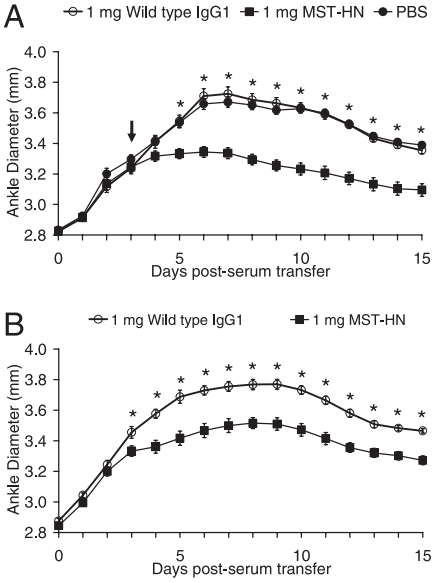

FIGURE 4. MST-HN is effective in ameliorating arthritis both during ongoing disease and prophylactically. *A*, To treat established disease, BALB/c mice were injected on day 0 with arthritogenic serum and 72 h later (indicated by arrow) treated with 1 mg MST-HN, 1 mg wild-type IgG1, or PBS (n = 7–8 mice per treatment group). Ankle swelling was not significantly different between wild-type IgG1- and PBS-treated mice, whereas MST-HN treatment significantly reduced swelling with respect to wild-type IgG1 or PBS treatment from day 5 onward ($*p < 2 \times 10^{-4}$, day 5; all $p < 7 \times 10^{-8}$, day 6 onward; ANOVA). *B*, BALB/c mice were treated with 1 mg MST-HN or 1 mg wild-type IgG1 (n = 6 mice per treatment group) 12 h prior to K/B×N serum transfer (day 0). Ankle swelling was significantly lower (*) in mice treated with MST-HN compared with wild-type IgG1-treated mice from day 3 onward (Student t test: $p < 3 \times 10^{-2}$, day 3; $p < 4 \times 10^{-3}$, day 4; $p < 8 \times 10^{-5}$, day 5; $p < 2 \times 10^{-4}$, day 6; all $p < 9 \times 10^{-5}$, day 7 onward).

data demonstrate that at a dose of 0.5 or 1 mg per mouse, wild-type IgG1 has no therapeutic activity (Fig. 3*A*, 3*B*), suggesting that the disease amelioration induced by the same doses of MST-HN involves FcRn inhibition.

To further investigate the FcRn dependence of MST-HN activity, the impact of MST-HN delivery on the clearance of ^{125}I-radiolabeled mouse IgG1 in FcRn knockout mice (34) was examined. No significant difference in the $t_{1/2}$ of radiolabeled IgG1 was observed in mice treated with either 1 mg MST-HN (30.4 h ± 1.15, SEM, n = 5 mice) or 1 mg wild-type IgG1 (32.2 h ± 1.05, SEM, n = 5 mice). These results are therefore consistent with the concept that a primary mechanism of Abdeg action is through FcRn inhibition.

MST-HN treatment does not downregulate FcRn

In addition to the well-established role of FcRn in regulating IgG levels (14, 15), it also functions to transport and recycle albumin

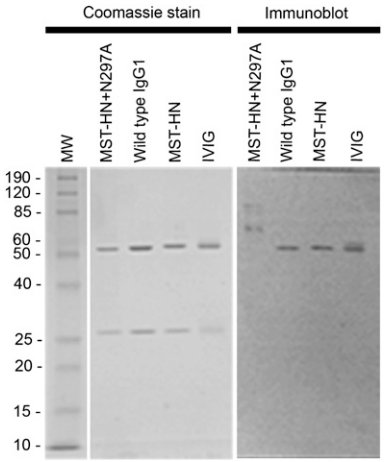

FIGURE 5. Immunoblotting analyses of human IgGs using SNA. A total of 1 μg each of MST-HN + N297A (aglycosylated MST-HN), wild-type human IgG1, MST-HN, and IVIG was electrophoresed on 12% SDS polyacrylamide gels and either stained with Coomassie brilliant blue or transferred onto a polyvinylidene difluoride membrane for immunoblotting. Sizes of m.w. standards (MW) are indicated in kDa on the *left margin*.

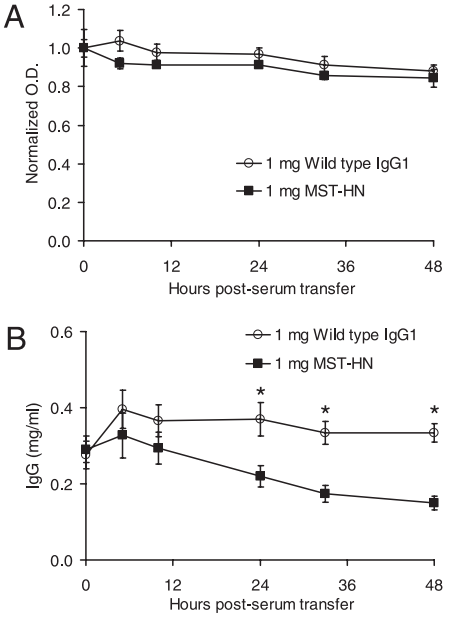

FIGURE 6. MST-HN does not affect serum albumin levels and lowers total IgG in mice. BALB/c mice were treated with 1 mg MST-HN or 1 mg wild-type IgG1 6 h following K/B×N serum transfer, using the protocol described in Fig. 3*B*. *A*, Serum albumin levels were determined by ELISA and were not significantly different (Student *t* test) between mice treated with MST-HN and wild-type IgG1 ($n = 5$ and 6 mice per treatment group, respectively; duplicate samples for each mouse). *B*, Total serum IgG levels were determined by ELISA for the same treatment groups as in *A*, and were significantly lower (*) in mice treated with MST-HN relative to those treated with wild-type IgG1 (Student *t* test: $p = 6.8 \times 10^{-3}$, 24 h; $p = 3.3 \times 10^{-3}$, 33 h; $p = 1 \times 10^{-4}$, 48 h). Error bars indicate SEM. Data are representative of at least two independent experiments.

(41). The lack of overlap between the IgG and albumin binding sites on FcRn (42) has enabled us to use albumin levels to assess whether the MST-HN mutant impacts FcRn expression and/or downregulation. For example, it is conceivable that through high-affinity, bivalent binding to FcRn, MST-HN might promote lysosomal trafficking of this receptor. Importantly, albumin levels did not vary significantly between different treatment groups, whereas total IgG levels decrease (Fig. 6). These data demonstrate that the MST-HN mutant acts through competition with endogenous IgGs for binding to FcRn in the absence of significant effects on FcRn downregulation/degradation.

MST-HN is as effective as 25- to 50-fold higher doses of IVIG in treating arthritis

Comparison of the impact of 1 mg MST-HN and 1 mg IVIG on arthritis indicated that, by contrast with MST-HN, 1 mg IVIG had no significant therapeutic effect (data not shown). This result is not unexpected, because IVIG comprises primarily human IgG1, which at this low dose also does not alter disease incidence and severity (Fig. 3*B*). We therefore determined the dose of IVIG necessary to induce similar therapeutic effects as 1 mg MST-HN. Mice were treated with 1 mg MST-HN, 25 mg IVIG, 50 mg IVIG, or, as control, 1 mg wild-type IgG1, and disease activity was monitored (Fig. 7*A*). The reduction in ankle swelling in mice treated with 1 mg MST-HN was between that induced by 25 and 50 mg IVIG (~1250 and 2500 mg/kg, respectively), although differences between MST-HN and IVIG treatment groups were not significant. Similar results were observed for paw swelling (data not shown). Consequently, ~25- to 50-fold more IVIG is needed to induce the therapeutic benefit that is achievable with 1 mg MST-HN. Consistent with the observations in Fig. 3*B* and 3*D*, disease severity correlated with the amount of anti-GPI Abs present (Fig. 7*B*). In addition, MST-HN and IVIG lowered levels of competing mouse IgG1 under noninflammatory conditions in vivo (Fig. 7*C*).

Discussion

Recent interest has focused on targeting the humoral arm of the immune response for the treatment of many autoimmune diseases (1, 2). In the current study, we demonstrate that recombinant Abs of the Abdeg class can be used as an effective therapeutic to treat ongoing disease in the K/B×N serum transfer model of Ab-mediated arthritis. Consistent with the ability of Abdegs to inhibit FcRn, disease blockade is accompanied by a reduction in serum anti-GPI levels. Abdegs therefore have considerable promise as therapeutic reagents for IgG-mediated autoimmunity.

Although IVIG is currently used to treat a number of autoimmune diseases, high doses (~1–2 g/kg) are needed for efficacy (6, 43). This poses a challenge for use in the clinic that is exacerbated by the worldwide shortage of IVIG (9). In addition, the delivery of IVIG can result in adverse side effects due to the polyclonal nature of this therapeutic and immune complex-mediated damage (7, 8). These shortcomings have prompted the development of alternative approaches, such as the use of Fc-engineered Abs that bind with increased affinity to FcRn at endosomal pH and have longer in vivo $t_{1/2}$ (11). Delivery of these Abs alleviates autoimmunity in a murine model involving the passive transfer of human Abs from arthritic patients (11). Abs of this class compete poorly for FcRn due to the need for fluid-phase uptake into cells, and consequently, they require high and repeated dosing to show efficacy. Another strategy that has shown beneficial effects in a rat model of myasthenia gravis is to use Abs that block FcRn by binding through their variable domains (12). However, such Abs bind to FcRn with similarly high affinity at both pH 6.0 and 7.4, resulting in short in vivo $t_{1/2}$ and the need for repeat and frequent dosing (12).

An alternative approach that is described in this work is to use Fc engineering to generate Abdegs that bind through their Fc region with high affinity to FcRn in the pH range 6.0–7.4 (10). Consequently, relative to their wild-type counterparts, Abdegs accumulate in cells to higher concentrations through receptor-mediated uptake, where they outcompete wild-type IgGs for FcRn binding in endosomes (10, 25, 28). Nevertheless, due to the intrinsic pH

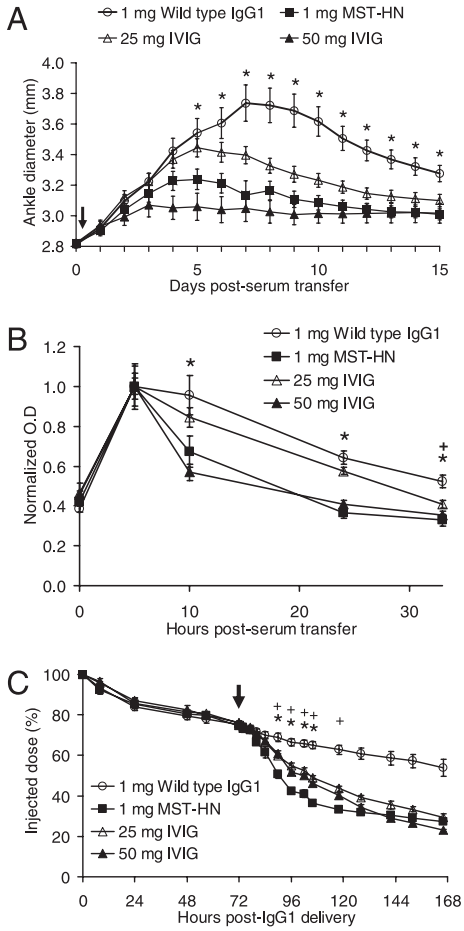

FIGURE 7. MST-HN has the same therapeutic effects as 25- to 50-fold higher doses of IVIG. *A*, BALB/c mice were injected on day 0 with arthritogenic serum and 6 h later (indicated by arrow) treated with 1 mg wild-type IgG1 ($n = 7$ mice), 1 mg MST-HN ($n = 7$ mice), 25 mg IVIG ($n = 6$ mice), or 50 mg IVIG ($n = 5$ mice), and disease monitored as in Fig. 3*A* and 3*B*. Relative to mice treated with 1 mg wild-type IgG1, disease activity was significantly lower in mice treated with 1 mg MST-HN (all $p < 5 \times 10^{-4}$, day 5 onward; ANOVA, *), 25 mg IVIG (all $p < 4 \times 10^{-4}$, day 7 onward; ANOVA), and 50 mg IVIG ($p < 4 \times 10^{-3}$, day 4; all $p < 5 \times 10^{-4}$, day 5 onward; ANOVA). No significant differences were observed between mice treated with MST-HN and either 25 or 50 mg IVIG. Disease activity was significantly different between the 25 and 50 mg IVIG treatment groups from days 4 to 6 ($p < 4 \times 10^{-3}$, ANOVA). *B*, Mice were treated as described in *A*, and anti-GPI Ab levels in sera of mice ($n = 4$ mice per treatment group; triplicate samples for each mouse) were determined by ELISA. Serum anti-GPI levels were significantly lower in mice treated with 1 mg MST-HN or 50 mg IVIG (*) and 25 mg IVIG (+) compared with mice treated with wild-type IgG1 ($p = 2.5 \times 10^{-3}$, 10 h; $p = 1 \times 10^{-4}$, 24 h; $p = 2.3 \times 10^{-3}$, 33 h; ANOVA). *C*, BALB/c mice were injected with ^{125}I-labeled mouse IgG1, as described in Fig. 1. After 72 h (indicated by arrow), mice were injected i.v. with either 1 mg wild-type IgG1 or MST-HN, or 25 or 50 mg IVIG ($n = 4$ mice per treatment group). Levels of remaining radiolabeled mouse IgG1 were determined by whole-body counting at the indicated times. Radioactivity levels were significantly lower for all treatment groups relative to wild-type IgG1 from 90 to 166 h ($p < 2 \times 10^{-4}$, 90 h; $p < 7 \times 10^{-6}$, 96–166 h; ANOVA). Relative to the 1 mg MST-HN treatment group, radioactivity levels were significantly higher in mice treated with 25 mg IVIG ($+p < 2 \times 10^{-4}$, 90 h; $p < 7 \times 10^{-6}$, 96–118 h; ANOVA) or 50 mg IVIG ($*p < 2 \times 10^{-4}$, 90 h; $p < 7 \times 10^{-6}$, 96–106 h; ANOVA). No significant difference was observed between the 25 and 50 mg IVIG treatment groups. Error bars indicate SEM. Data are representative of two independent experiments.

dependence of FcRn–IgG interactions (27, 44), Abs of the Abdeg class such as MST-HN retain significantly lower affinity at pH 7.4 relative to pH 6.0 (10). Consequently, MST-HN persists with a $t_{1/2}$ in mice of ~40 h (38), providing a significant advantage over the therapeutic use of shorter-lived Abs that bind to FcRn through their V regions (12, 17). Indeed, the available knowledge concerning how FcRn–IgG interaction properties impact the $t_{1/2}$ and FcRn-blocking activity of an Abdeg enables the optimization of Abdeg behavior for different applications (16, 25).

In the current study, treatment of mice 6 h following K/B×N serum transfer with a single dose of either 0.5 or 1 mg Abdeg ameliorates arthritis, with the higher dose resulting in maximal competitive effects and almost complete ablation of disease symptoms. By comparison with Abdeg, our studies show that 25- to 50-fold higher concentrations of IVIG are required to induce a comparable reduction in disease activity. Thus, the binding properties of Abdegs translate into potent therapeutic effects. Importantly, MST-HN delivery 72 h postserum transfer reduces disease activity when joints are visibly swollen, demonstrating therapeutic benefit in established disease. The potency of the Abdeg in reducing arthritis, however, was not as pronounced when administered prophylactically (12 h prior to K/B×N serum transfer) compared with delivery at 6 h postserum transfer. This observation is consistent with the relatively short $t_{1/2}$ of MST-HN (38), which is expected to render the prophylactically delivered Abdeg less effective in competing with anti-GPI Abs for FcRn binding.

Although in earlier studies the stoichiometry of FcRn binding to Fc (IgG) was uncertain, it is now established that the interaction comprises an asymmetric 2:1 FcRn:Fc (or IgG) complex (45–47). Relative to their homodimeric counterparts, heterodimeric Fc fragments with only one functional FcRn interaction site have shorter in vivo $t_{1/2}$ and are recycled less efficiently (48, 49). This, combined with our recent observations demonstrating that Abdegs enter the lysosomal pathway in cells (28), raises the question as to whether the presence of two relatively high-affinity binding sites on an Abdeg for FcRn could decrease recycling activity by diverting this receptor into lysosomes. In addition to transporting IgG, FcRn recycles serum albumin (41), a protein that is critical in maintaining oncotic pressure, blood pH, and transporting a range of small molecules. Importantly, the binding sites for albumin and IgG on FcRn are distinct (42). We therefore reasoned that by monitoring albumin levels, we could determine whether FcRn expression and/or intracellular trafficking were affected by Abdeg treatment. Our studies demonstrate that Abdegs function specifically through blocking FcRn–IgG interactions, and do not alter FcRn expression or distribution to impact albumin levels. The specificity of Abdeg effects for IgG indicates that the application of these reagents in the clinic will not result in the undesirable side effect of altering albumin homeostasis.

A question of direct relevance to the design of therapeutics is whether FcRn blockade alone is sufficient to treat Ab-mediated disease. For example, sialylation (α2,6-linked sialic acid) present on 1–3% of IgG molecules in IVIG has been shown to induce anti-inflammatory effects by upregulating FcγRIIB (21, 40). This upregulation has been reported to be either an important, or the sole, contributing factor to the therapeutic benefit of IVIG in the K/B×N serum transfer model (20, 21, 24). Our immunoblotting data indicate that the levels of α2,6-linked sialic acid on MST-HN or wild-type IgG1 are analogous to those present on IVIG, although the possibility of cross-reactivity of SNA with different forms of sialic/neuraminic acid on the recombinant Abs cannot be excluded (50). We therefore reasoned that comparison of the effects of the delivery of MST-HN and wild-type IgG1 on arthritis would enable us to assess the role of FcRn inhibition versus other possible anti-inflammatory pathways on the therapeutic effects of the Abdeg. Significantly, at the low doses (~25–50 mg/kg) of

recombinant Abs used in this study, wild-type IgG1 delivery does not modulate arthritis, suggesting that a primary mode of action of the MST-HN mutant is through FcRn blockade. This is also consistent with the inactivity of MST-HN in further reducing the $t_{1/2}$ of IgG in FcRn knockout mice, combined with the relationship between therapeutic efficacy and the ability of MST-HN or relatively high doses of IVIG to decrease Ab levels in vivo.

In the current study, we show that the use of Abs of the Abdeg class offers advantages over alternative approaches, including the ability of relatively low, single doses to treat disease when delivered following the initiation of immune complex-mediated inflammation. Collectively, our observations demonstrate that Abdegs represent highly efficacious and specific therapeutics that could have broad applicability in the management of IgG-mediated autoimmunity.

Acknowledgments

We thank Drs. Christophe Benoist and Diane Mathis for generously providing KRN transgenic mice. We are indebted to Dr. James Richardson and John Shelton (Molecular Pathology Core, University of Texas Southwestern Medical Center) for histologic preparations. We are grateful to Dr. Sripad Ram for expert advice on statistical analysis, Dr. Wentao Mi for advice on mouse husbandry, and Tom Lo for assistance.

Disclosures

E.S.W. is an inventor on a pending patent describing the use of Abdegs as FcRn inhibitors. The other authors have no financial conflicts of interest.

References

1. Sanz, I., F. E. Lee; Medscape. 2010. B cells as therapeutic targets in SLE. *Nat. Rev. Rheumatol.* 6: 326–337.
2. Tedder, T. F. 2009. CD19: a promising B cell target for rheumatoid arthritis. *Nat. Rev. Rheumatol.* 5: 572–577.
3. Sathasivam, S. 2008. Steroids and immunosuppressant drugs in myasthenia gravis. *Nat. Clin. Pract. Neurol.* 4: 317–327.
4. Schieppati, A., and G. Remuzzi. 2008. Novel therapies of lupus nephritis. *Curr. Opin. Nephrol. Hypertens.* 17: 156–161.
5. Kazatchkine, M. D., and S. V. Kaveri. 2001. Immunomodulation of autoimmune and inflammatory diseases with intravenous immune globulin. *N. Engl. J. Med.* 345: 747–755.
6. Stangel, M., and R. Pul. 2006. Basic principles of intravenous immunoglobulin (IVIg) treatment. *J. Neurol.* 253(Suppl. 5): V18–V24.
7. Ballow, M. 1991. Mechanisms of action of intravenous immunoglobulin therapy and potential use in autoimmune connective tissue diseases. *Cancer* 68: 1430–1436.
8. Kessary-Shoham, H., Y. Levy, Y. Shoenfeld, M. Lorber, and H. Gershon. 1999. In vivo administration of intravenous immunoglobulin (IVIg) can lead to enhanced erythrocyte sequestration. *J. Autoimmun.* 13: 129–135.
9. Bayry, J., M. D. Kazatchkine, and S. V. Kaveri. 2007. Shortage of human intravenous immunoglobulin: reasons and possible solutions. *Nat. Clin. Pract. Neurol.* 3: 120–121.
10. Vaccaro, C., J. Zhou, R. J. Ober, and E. S. Ward. 2005. Engineering the Fc region of immunoglobulin G to modulate in vivo antibody levels. *Nat. Biotechnol.* 23: 1283–1288.
11. Petkova, S. B., S. Akilesh, T. J. Sproule, G. J. Christianson, H. Al Khabbaz, A. C. Brown, L. G. Presta, Y. G. Meng, and D. C. Roopenian. 2006. Enhanced half-life of genetically engineered human IgG1 antibodies in a humanized FcRn mouse model: potential application in humorally mediated autoimmune disease. *Int. Immunol.* 18: 1759–1769.
12. Liu, L., A. M. Garcia, H. Santoro, Y. Zhang, K. McDonnell, J. Dumont, and A. Bitonti. 2007. Amelioration of experimental autoimmune myasthenia gravis in rats by neonatal FcR blockade. *J. Immunol.* 178: 5390–5398.
13. Huang, H., C. Benoist, and D. Mathis. 2010. Rituximab specifically depletes short-lived autoreactive plasma cells in a mouse model of inflammatory arthritis. *Proc. Natl. Acad. Sci. USA* 107: 4658–4663.
14. Ghetie, V., J. G. Hubbard, J. K. Kim, M. F. Tsen, Y. Lee, and E. S. Ward. 1996. Abnormally short serum half-lives of IgG in beta 2-microglobulin-deficient mice. *Eur. J. Immunol.* 26: 690–696.
15. Junghans, R. P., and C. L. Anderson. 1996. The protection receptor for IgG catabolism is the beta2-microglobulin-containing neonatal intestinal transport receptor. *Proc. Natl. Acad. Sci. USA* 93: 5512–5516.
16. Ward, E. S., and R. J. Ober. 2009. Multitasking by exploitation of intracellular transport functions: the many faces of FcRn. *Adv. Immunol.* 103: 77–115.
17. Getman, K. E., and J. P. Balthasar. 2005. Pharmacokinetic effects of 4C9, an anti-FcRn antibody, in rats: implications for the use of FcRn inhibitors for the treatment of humoral autoimmune and alloimmune conditions. *J. Pharm. Sci.* 94: 718–729.
18. Mezo, A. R., K. A. McDonnell, C. A. Hehir, S. C. Low, V. J. Palombella, J. M. Stattel, G. D. Kamphaus, C. Fraley, Y. Zhang, J. A. Dumont, and A. J. Bitonti. 2008. Reduction of IgG in nonhuman primates by a peptide antagonist of the neonatal Fc receptor FcRn. *Proc. Natl. Acad. Sci. USA* 105: 2337–2342.
19. Hansen, R. J., and J. P. Balthasar. 2002. Effects of intravenous immunoglobulin on platelet count and antiplatelet antibody disposition in a rat model of immune thrombocytopenia. *Blood* 100: 2087–2093.
20. Samuelsson, A., T. L. Towers, and J. V. Ravetch. 2001. Anti-inflammatory activity of IVIG mediated through the inhibitory Fc receptor. *Science* 291: 484–486.
21. Kaneko, Y., F. Nimmerjahn, and J. V. Ravetch. 2006. Anti-inflammatory activity of immunoglobulin G resulting from Fc sialylation. *Science* 313: 670–673.
22. Bleeker, W. K., J. L. Teeling, and C. E. Hack. 2001. Accelerated autoantibody clearance by intravenous immunoglobulin therapy: studies in experimental models to determine the magnitude and time course of the effect. *Blood* 98: 3136–3142.
23. Li, N., M. Zhao, J. Hilario-Vargas, P. Prisayanh, S. Warren, L. A. Diaz, D. C. Roopenian, and Z. Liu. 2005. Complete FcRn dependence for intravenous Ig therapy in autoimmune skin blistering diseases. *J. Clin. Invest.* 115: 3440–3450.
24. Akilesh, S., S. Petkova, T. J. Sproule, D. J. Shaffer, G. J. Christianson, and D. Roopenian. 2004. The MHC class I-like Fc receptor promotes humorally mediated autoimmune disease. *J. Clin. Invest.* 113: 1328–1333.
25. Vaccaro, C., R. Bawdon, S. Wanjie, R. J. Ober, and E. S. Ward. 2006. Divergent activities of an engineered antibody in murine and human systems have implications for therapeutic antibodies. *Proc. Natl. Acad. Sci. USA* 103: 18709–18714.
26. Ram, S., P. Prabhat, J. Chao, E. S. Ward, and R. J. Ober. 2008. High accuracy 3D quantum dot tracking with multifocal plane microscopy for the study of fast intracellular dynamics in live cells. *Biophys. J.* 95: 6025–6043.
27. Dall'Acqua, W. F., R. M. Woods, E. S. Ward, S. R. Palaszynski, N. K. Patel, Y. A. Brewah, H. Wu, P. A. Kiener, and S. Langermann. 2002. Increasing the affinity of a human IgG1 for the neonatal Fc receptor: biological consequences. *J. Immunol.* 169: 5171–5180.
28. Gan, Z., S. Ram, C. Vaccaro, R. J. Ober, and E. S. Ward. 2009. Analyses of the recycling receptor, FcRn, in live cells reveal novel pathways for lysosomal delivery. *Traffic* 10: 600–614.
29. Kouskoff, V., A. S. Korganow, V. Duchatelle, C. Degott, C. Benoist, and D. Mathis. 1996. Organ-specific disease provoked by systemic autoimmunity. *Cell* 87: 811–822.
30. Ji, H., K. Ohmura, U. Mahmood, D. M. Lee, F. M. Hofhuis, S. A. Boackle, K. Takahashi, V. M. Holers, M. Walport, C. Gerard, et al. 2002. Arthritis critically dependent on innate immune system players. *Immunity* 16: 157–168.
31. Korganow, A. S., H. Ji, S. Mangialaio, V. Duchatelle, R. Pelanda, T. Martin, C. Degott, H. Kikutani, K. Rajewsky, J. L. Pasquali, et al. 1999. From systemic T cell self-reactivity to organ-specific autoimmune disease via immunoglobulins. *Immunity* 10: 451–461.
32. Maccioni, M., G. Zeder-Lutz, H. Huang, C. Ebel, P. Gerber, J. Hergueux, P. Marchal, V. Duchatelle, C. Degott, M. van Regenmortel, et al. 2002. Arthritogenic monoclonal antibodies from K/B×N mice. *J. Exp. Med.* 195: 1071–1077.
33. Wipke, B. T., Z. Wang, J. Kim, T. J. McCarthy, and P. M. Allen. 2002. Dynamic visualization of a joint-specific autoimmune response through positron emission tomography. *Nat. Immunol.* 3: 366–372.
34. Roopenian, D. C., G. J. Christianson, T. J. Sproule, A. C. Brown, S. Akilesh, N. Jung, S. Petkova, L. Avanessian, E. Y. Choi, D. J. Shaffer, et al. 2003. The MHC class I-like IgG receptor controls perinatal IgG transport, IgG homeostasis, and fate of IgG-Fc-coupled drugs. *J. Immunol.* 170: 3528–3533.
35. Foote, J., and G. Winter. 1992. Antibody framework residues affecting the conformation of the hypervariable loops. *J. Mol. Biol.* 224: 487–499.
36. Zhou, J., F. Mateos, R. J. Ober, and E. S. Ward. 2005. Conferring the binding properties of the mouse MHC class I-related receptor, FcRn, onto the human ortholog by sequential rounds of site-directed mutagenesis. *J. Mol. Biol.* 345: 1071–1081.
37. Amit, A. G., R. A. Mariuzza, S. E. Phillips, and R. J. Poljak. 1986. Three-dimensional structure of an antigen-antibody complex at 2.8 Å resolution. *Science* 233: 747–753.
38. Montoyo, H. P., C. Vaccaro, M. Hafner, R. J. Ober, W. Mueller, and E. S. Ward. 2009. Conditional deletion of the MHC class I-related receptor FcRn reveals the sites of IgG homeostasis in mice. *Proc. Natl. Acad. Sci. USA* 106: 2788–2793.
39. Ji, H., D. Gauguier, K. Ohmura, A. Gonzalez, V. Duchatelle, P. Danoy, H. J. Garchon, C. Degott, M. Lathrop, C. Benoist, and D. Mathis. 2001. Genetic influences on the end-stage effector phase of arthritis. *J. Exp. Med.* 194: 321–330.
40. Anthony, R. M., F. Nimmerjahn, D. J. Ashline, V. N. Reinhold, J. C. Paulson, and J. V. Ravetch. 2008. Recapitulation of IVIG anti-inflammatory activity with a recombinant IgG Fc. *Science* 320: 373–376.
41. Chaudhury, C., S. Mehnaz, J. M. Robinson, W. L. Hayton, D. K. Pearl, D. C. Roopenian, and C. L. Anderson. 2003. The major histocompatibility complex-related Fc receptor for IgG (FcRn) binds albumin and prolongs its lifespan. *J. Exp. Med.* 197: 315–322.
42. Andersen, J. T., J. Dee Qian, and I. Sandlie. 2006. The conserved histidine 166 residue of the human neonatal Fc receptor heavy chain is critical for the pH-dependent binding to albumin. *Eur. J. Immunol.* 36: 3044–3051.
43. Blumberg, R. S., and W. I. Lencer. 2005. Antibodies in the breakdown lane. *Nat. Biotechnol.* 23: 1232–1234.

44. Raghavan, M., V. R. Bonagura, S. L. Morrison, and P. J. Bjorkman. 1995. Analysis of the pH dependence of the neonatal Fc receptor/immunoglobulin G interaction using antibody and receptor variants. *Biochemistry* 34: 14649–14657.
45. Martin, W. L., and P. J. Bjorkman. 1999. Characterization of the 2:1 complex between the class I MHC-related Fc receptor and its Fc ligand in solution. *Biochemistry* 38: 12639–12647.
46. Schuck, P., C. G. Radu, and E. S. Ward. 1999. Sedimentation equilibrium analysis of recombinant mouse FcRn with murine IgG1. *Mol. Immunol.* 36: 1117–1125.
47. Sánchez, L. M., D. M. Penny, and P. J. Bjorkman. 1999. Stoichiometry of the interaction between the major histocompatibility complex-related Fc receptor and its Fc ligand. *Biochemistry* 38: 9471–9476.
48. Kim, J. K., M. F. Tsen, V. Ghetie, and E. S. Ward. 1994. Catabolism of the murine IgG1 molecule: evidence that both CH2-CH3 domain interfaces are required for persistence of IgG1 in the circulation of mice. *Scand. J. Immunol.* 40: 457–465.
49. Tesar, D. B., N. E. Tiangco, and P. J. Bjorkman. 2006. Ligand valency affects transcytosis, recycling and intracellular trafficking mediated by the neonatal Fc receptor. *Traffic* 7: 1127–1142.
50. Shibuya, N., I. J. Goldstein, W. F. Broekaert, M. Nsimba-Lubaki, B. Peeters, and W. J. Peumans. 1987. The elderberry (*Sambucus nigra* L.) bark lectin recognizes the Neu5Ac(alpha 2-6)Gal/GalNAc sequence. *J. Biol. Chem.* 262: 1596–1601.